Therapeutic arteriogenesis by factor-decorated fibrin matrices promotes wound healing in diabetic mice

**Rosalinda D'Amico[1,2]*, Camilla Malucelli[1]*, Andrea Uccelli[1],
Andrea Grosso[1], Nunzia Di Maggio[1], Priscilla S Briquez[3],
Jeffrey A Hubbell[3], Thomas Wolff[2], Lorenz Gürke[2], Edin Mujagic[2],
Roberto Gianni-Barrera[1]*** (ID) **and Andrea Banfi[1,2]*** (ID)

Abstract
Chronic wounds in type-2 diabetic patients present areas of severe local skin ischemia despite mostly normal blood flow in deeper large arteries. Therefore, restoration of blood perfusion requires the opening of arterial connections from the deep vessels to the superficial skin layer, that is, arteriogenesis. Arteriogenesis is regulated differently from microvascular angiogenesis and is optimally stimulated by high doses of Vascular Endothelial Growth Factor-A (VEGF) together with Platelet-Derived Growth Factor-BB (PDGF-BB). Here we found that fibrin hydrogels decorated with engineered versions of VEGF and PDGF-BB proteins, to ensure protection from degradation and controlled delivery, efficiently accelerated wound closure in diabetic and obese db/db mice, promoting robust microvascular growth and a marked increase in feeding arterioles. Notably, targeting the arteriogenic factors to the intact arterio-venous networks in the dermis around the wound was more effective than the routine treatment of the inflamed wound bed. This approach is readily translatable to a clinical setting.

Keywords
Wound-healing, arteriogenesis, angiogenesis, VEGF, PDGF-BB, fibrin

Introduction

An estimated 463 million people were living with diabetes in 2019 and this number is expected to reach 700 million by 2045,[1] making diabetes a major global health emergency. Obesity-associated type 2 diabetes mellitus (DM2) accounts for around 90% of all diabetes cases worldwide.[1] Diabetic foot ulcers (DFU) are a common secondary complication of DM2,[2] with a recurrence rate of 65% within 5 years[3] and very serious sequelae, often necessitating amputation[1] and even leading to death.[4] Diabetic hyperglycemia has been implicated in the progression of vascular disease in both animal and clinical studies.[5] In particular, deficient angiogenesis during the wound healing process causes areas of local skin ischemia and severely impaired blood flow, which profoundly delay re-epithelialization by resident epidermal stem cells.[6]

Attempts at improving the perfusion of chronic wounds in diabetic patients have focused on both vasculogenesis,

[1]Cell and Gene Therapy, Department of Biomedicine, Basel University Hospital and University of Basel, Basel, Switzerland
[2]Vascular Surgery, Department of Surgery, Basel University Hospital and University of Basel, Basel, Switzerland
[3]Pritzker School of Molecular Engineering, University of Chicago, Chicago, IL, USA

*These authors have contributed equally to this work.

Corresponding authors:
Andrea Banfi, Cell and Gene Therapy, Department of Biomedicine, Basel University Hospital, Hebelstrasse 20, Basel 4056, Switzerland.
Email: Andrea.Banfi@usb.ch

Roberto Gianni-Barrera, Cell and Gene Therapy, Department of Biomedicine, Basel University Hospital, Hebelstrasse 20, Basel 4056, Switzerland.
Email: Roberto.GianniBarrera@usb.ch

which relies on the *in-situ* recruitment of endothelial progenitor cells (EPCs), and therapeutic angio-genesis, that is, the stimulation of microvascular growth in the damaged tissue. This has been attempted either by topical application of growth factors such as VEGF[6] or of mesenchymal stem cells (MSCs), which produce several paracrine factors that promote angiogenesis and granulation tissue formation in wounded tissues.[7]

In contrast, therapeutic arterio-genesis is the induction of new functional feeding arteries through the enlargement and remodeling of small non-perfused pre-existing vessels and is necessary to restore functional perfusion of ischemic tissue. The process of arteriogenesis is regulated through different mechanisms from angiogenesis, though the two are functionally connected.[8] In fact, angiogenesis is best promoted by moderate doses of VEGF alone, whereas arteriogenesis is optimally stimulated by higher doses of VEGF together with PDGF-BB, which regulates the recruitment of pericytes and smooth muscle cells to newly formed vessels.[9] In particular it was shown that coordinated co-delivery of both growth factors at an optimal ratio: (1) improved both collateral arteriogenesis and blood flow in a murine hindlimb ischemia model[10] and (2) stimulated robust arteriogenesis, coupled to expanded microvascular capillary networks, both in murine skeletal muscle[11] and murine diabetic skin.[12]

Therefore, here we investigated the potential of therapeutic arteriogenesis for diabetic wound healing by biomaterial-based controlled co-delivery of a high dose of engineered VEGF and PDGF-BB proteins. BKS. Cg-Dock7^m+/+Lepr^{db}/J mice (db/db mice) were used, as they spontaneously develop insulin resistance, diabetes and morbid obesity, and are the gold-standard model for DM2.[13]

In order to protect the growth factors as much as possible from proteolytic degradation in the wound environment, we took advantage of a fibrin-based delivery platform that we previously optimized,[14] whereby engineered versions of the therapeutic proteins are fused to the transglutaminase substrate octapeptide NQEQVSPL (TG-VEGF and TG-PDGF-BB), to allow its covalent cross-linking into fibrin hydrogels by the coagulation factor XIIIa and release only by enzymatic cleavage. In clinical practice wound treatments are commonly applied directly to the wound bed.[15,16] However, two factors could limit the efficacy of arteriogenic treatment in the wound bed: (1) the inflammatory environment, rich in proteolytic enzymes that accelerate the degradation of protein factors[17]; and (2) the fact that the feeding arterio-venous network, which runs in the hypodermic layer of the skin, is also destroyed under the wound bed. Therefore, we investigated whether an arteriogenic treatment would be most effective if applied by injection into the intact hypodermic layer around the wound rather than by layering on the wound bed itself.

Materials and methods

BKS.Cg-Dock7m+/+Leprdb/J (db/db) mice

Heterozygous mice of a spontaneous genetic mouse model of DM2 (BKS.Cg-Dock7m+/+Leprdb/J (db/db) diabetic and obese murine strain) were purchased from Jackson Laboratory (Bar Harbor, ME, USA) to produce a local colony. Blood glucose levels and body weights were systematically measured once per week from the age of 8 till 10 weeks, when animals entered the experiment. Blood glucose levels were measured on tail-vein blood samples with a glucose meter (Ascensia Diabetes, Basel, Switzerland). Additionally, all animal were genotyped according to a protocol by the Jackson Laboratory, using the following primers in the *Lepr* gene: IMR0985 (Forward): 5′–AGAACGGACACTCTTTGAAGTCTC–3′ and IMR0986 (Reverse): 5′–CATTCAAACCATAGTTTA GGTTTGTGT–3′. The DNA amplicon was digested with RsaI (Bioconcept, Allschwil, Switzerland) and separated on a 2.75% Ethidium Bromide-stained agarose gel. Two bands of 108 bp and 27 bp identified the homozygous db/db mice, a single 135 bp band the wild-type mice and the presence of all three bands the heterozygous mice. Additionally, male mice displayed a further band of 170 bp.

Recombinant murine TG-VEGF$_{164}$ and TG-PDGF-BB production

Recombinant mouse TG-VEGF$_{164}$ and mouse TG-PDGF-BB were produced as previously described.[12,14] Briefly, VEGF and PDGF-BB were engineered at their N-terminus with the NQEQVSPL octapeptide, to allow their covalent cross-linking into fibrin hydrogels. Fusion proteins were expressed into the *Escherichia coli* strain BL21 (Dε3) pLys (Novagen, Madison, WI, USA) and isolated as previously described.[12,14,18] Once produced, TG-VEGF and TG-PDGF-BB dimers were verified to be >99% pure by SDS/PAGE. Endotoxin level was verified to be under 0.05 EU/mg of protein using the human embryonic kidney (HEK)-Blue mTLR4 assay (Invivogen, San Diego, California, USA).

Fibrin gels

Fibrin matrices were prepared by mixing human fibrinogen (plasminogen-, von Willebrand Factor-, and fibronectin-depleted; 25 mg/mL; Enzymes Research Laboratories, Indiana, USA), fluorescent Alexa 647-conjugated fibrinogen (0.5 mg/mL; Invitrogen, California, USA), factor XIIIa (3 U/mL; CSL Behring, Pennsylvania, USA), and thrombin (6 U/mL; Sigma-Aldrich, Missouri, USA) with 2.5 mM Ca^{2+} in 4-(2-hydroxyethyl)-1-piperazineethanesulfonic acid (Hepes) (Lonza, Basel, CH). Matrices containing TG-VEGF and TG-PDG-BB were obtained by adding the

engineered proteins to the cross-linking enzymes solution before mixing with fibrinogen.

Wounding and in vivo hydrogel delivery

Animals were treated in accordance with Swiss Federal guidelines for animal welfare and the study protocol was approved by the Veterinary Office of the Canton of Basel-Stadt (Basel, Switzerland, Permit 2952). Surgeries were carried out under sterile conditions. Equal proportions of male and female mice were used in each group, so as to avoid potential sex-related bias. Ten-week old db/db mice were anesthetized by a mixture of oxygen (0.6 L/min) and 2% Vol Isofluorane for induction and 1.5%–1.8% Vol for maintenance. Analgesia was ensured by subcutaneous injection of Buprenorphine (0.1 mg/kg/dose) 30 min before the surgery, as well as after 4 and 8 h and the next morning. Before surgery the dorsal skin was carefully disinfected by using a betadine solution (Mundipharma Medical Company, Basel, Switzerland). Two full-thickness punch biopsy wounds (6 mm in diameter) were performed on the dorsal skin. Immediately after surgery, a liquid volume of 50 µL fluorescent fibrin hydrogel, carrying a mixture of 100 µg/mL TG-VEGF and 10 µg/mL TG-PDGF-BB or no factors (control), was layered on the wound bed. Alternatively, fibrin hydrogels were divided in 4 or 8 individual liquid volume of 21.5 µL each, aspirated rapidly with a 0.3-mL insulin syringe with integrated $29^{1}/_{2}$G needle (Becton Dickinson, Allschwil, Switzerland) and injected into the dermal layer around the wounds. At the end of the procedure, wounds were covered with a transparent sterile occlusive dressing (3M, Rüschlikon, Switzerland), which was changed every other day when wound closure was measured, together with inspection for signs of inflammation, infection or necrosis. During this procedure, dorsal skin around the wound was carefully disinfected with betadine solution (Mundipharma Medical Company, Basel, Switzerland). After surgery, animals were housed individually to prevent wounding by other animals.

In vivo wound measurement

Three mice were used to determine the maximum feasible treatment dose to be layered on the wound beds without overflow and also to confirm histologically the correct presence of the layered fibrin matrices on the exposed wound bed and the intradermal location of the injected gels. These animals were euthanized 2 h after fibrin gel delivery. For the study of wound healing kinetics, 30 db/db mice were divided into groups of five animals/experimental condition (10 wounds) and were followed over time.

The percentage of wound closure over time was calculated as (1−[remaining wound area]/[initial wound area]). Since wounds displayed mostly an elliptical shape, areas were calculated from measuring the two mutually perpendicular major and minor radiuses by an electric digital caliper (Fisher Scientific, Reinach, Switzerland), starting from the day of wounding and every 2 days thereafter until the sacrifice time-points, in mice previously anesthetized with Isofluorane inhalation.

Tissue staining

For the studies performed on frozen and paraffin tissue sections, a separate set of 18 db/db mice were divided into groups of three animals/experimental condition (six wounds) and euthanized 7 days after treatment. Briefly, mice were anesthetized with i.p. Ketamine (100 mg/kg) and Xylazine (10 mg/kg) and sacrificed by intravascular perfusion of 1% paraformaldehyde in PBS pH 7.4 for 4 min under 120 mm/Hg of pressure. This was done to prevent vascular collapse upon termination of cardiac activity with loss of arterial pressure, and ensure reliable quantification of vascular diameters.[19] Skin wounds were carefully harvested including the deepest dermal layers, and divided into two equal halves by cutting them longitudinally along their major diameter. The cranial half was post-fixed in 0.5% paraformaldehyde in PBS for 2 h at room temperature, cryo-protected in 30% sucrose in PBS overnight at 4°C, embedded in OCT compound (CellPath, Newtown, Powys, UK), frozen in freezing isopentane and cryosectioned (35-µm sections). The caudal half was post-fixed in 1% paraformaldehyde in PBS overnight, washed with PBS twice and stored in ethanol 70% until samples were embedded in paraffin and sectioned (10-µm sections). All analyses were performed on sections taken from the widest central part of the wounds, which were unequivocally identified by the truncated muscle edges of the panniculus carnosus (PC) muscle after staining with hematoxylin and eosin (HE), as described previously.[20] Immunofluorescence staining was performed on 35 µm-thick frozen sections with the following primary antibodies and dilutions: rat monoclonal anti-mouse CD31 (clone MEC 13.3, BD Biosciences, Basel, Switzerland) at 1:100 (0.5 mg/mL), mouse monoclonal anti-mouse α-SMA (clone 1A4, MP Biomedicals, Basel, Switzerland) at 1:400 (71 µg/mL). Fluorescently labeled secondary antibodies (Invitrogen, Basel, Switzerland) were used at 1:200 (10 µg/mL) and DAPI (Merck KGaA, Darmstadt, Germany) at 1:50 (1 mg/mL).

Hystological analyses

All histological analyses were performed by two blinded and independent investigators to avoid bias. The extent of re-epithelialization was quantified on 10 µm-thick HE-stained sections as previously described.[21] Briefly, the interruptions of the PC muscle and of the corresponding dermis were used as indicators for the wound edges. The

distance between the two opposite dermis interruptions and the length covered by epithelium regeneration were measured. The ratio between the two measurements represent the percentage of wound closure.[21]

All quantifications of vascular growth were performed in standardized tissue areas either in the periphery or in the center of the wound defined as following: two peripheral areas/section, which extended 2 mm beyond each wound edge starting from the interruption of the PC muscle, and one area of 800-µm width covering the central portion of the wound. The height of these areas included all dermal layers.

Vessel length density (VLD) was quantified in fluorescently immunostained 35 µm-thick cryosections, as previously described.[12] Briefly, the vessel length was traced in all fields with a clear increased angiogenic activity (compared to nearby fields) within the three areas described above in each section ($n=4$ wounds/group) and was divided by the area of each identified field. VLD measurements were then averaged by the number of total analyzed tissue areas either in the periphery or in the center of the wound. The total vessel length was defined as the sum of vessel length of all the angiogenic fields within the standardized tissue areas per wound. The total angiogenic area was the sum of the areas of all angiogenic fields within the analyzed areas per wound.

The arterial density and total number of arterioles were quantified in fluorescently immunostained cryosections. Arterioles were defined as vessels of regular shape and larger than capillaries ($\geqslant 15 \mu m$) associated with a thick and homogeneous smooth muscle layer (positive for α-smooth muscle actin, α-SMA) coating the endothelial layer (positive for CD31), as previously described.[11,12] The number of arterioles was quantified an area of fixed size around each previously identified angiogenic area, extending beyond its edges by 500 µm in all directions. The absolute number of arterioles in each field was normalized by its analyzed area (arterial density), or summed together for a given sample (total number of arterioles) either in the center or in the periphery ($n=4$–6 wounds/group).

All images were taken with a 20× (numerical aperture=0.75) or a 10× (numerical aperture=0.45) objective on a Nikon Eclipse Ti2 microscope (Nikon, Egg/Zürich, Switzerland), or a 20× objective (numerical aperture=0.75) on a Nikon A1R laser scanning confocal microscope (Nikon, Egg/Zürich, Switzerland). Analyses were conducted with NIS-Elements Advanced Research software (Nikon, Egg/Zürich, Switzerland). 3D immunofluorescence images were generated with Imaris 9.1.2 software (Bitplane, Zürich, Switzerland).

Statistical analysis

Data are presented as means ± standard error. The significance of differences was assessed with the GraphPad Prism 9.1.2 software (GraphPad Software). The normal distribution of all data sets was determined by D'Agostino and Pearson or Shapiro-Wilk tests. Multiple comparisons were performed with parametric one-way analysis of variance (ANOVA) followed by the Holm-Sidak test for multiple comparisons, while single comparisons were analyzed with the parametric t-test. $p < 0.05$ was considered statistically significant.

Results

Calculation of equivalent dosing between wound layering or intradermal injection of fibrin matrices

Homozygous db/db mice were bred from heterozygous pairs and identified based on their genotype (Supplemental Figure S1a). Measurement of body weights and blood glucose levels confirmed that by the age of 8–10 weeks, all db/db animals which entered the experiments (male and female in about 1:1 ratio) were both obese and diabetic, whereas db/+ heterozygous littermate control mice had both physiologic weight and glycemia, as previously described[22,23] (Supplemental Figure S1b-c; body weight: db/+ = 25 ± 0.5 g vs db/db = 38.2 ± 0.5 g; glycemia: db/+ = 115.2 ± 5.0 mg/dL vs /db = 315.0 ± 9.1 mg/dL; $p < 0.0001$ for both comparisons).

To determine the maximum feasible treatment dose, it was found that, immediately after surgery, it was possible to layer a maximum volume of 50 µL of fibrin gel on the exposed wound bed without overflow (yellow arrows in Supplemental Figure S2a). Following the US Food and Drug Administration (FDA) guidelines,[24] we calculated the equivalent amount of fibrin gel to be injected around the wound rim, based on the surface area to be treated. The 6-mm full-thickness circular excisional wounds have a surface of about 9π mm^2. The surface area occupied by the ring of fibrin gel injections extended beyond the wound edge by 2 mm on average, equivalent to a surface of about 16π mm^2, that is about 1.7-fold the wound surface area. The equivalent dose to be injected around the wound rim was therefore calculated as $1.7 \times 50 \mu L = 85 \mu L$ of fibrin gel, which was divided in four individual volumes of 21.5 µL each and injected at the four cardinal points around the wound (yellow arrows in Supplemental Figure S2b). Animals were euthanized 2 h after injections or layering for histological verification, as it was previously shown that fibrin gels are fully polymerized at this stage,[12] and in order to avoid the processes of gel degradation and remodeling by host cells, which start at later time points.

Visualization of fluorescent fibrinogen together with immunofluorescence staining of endothelium (CD31), confirmed the correct presence of the layered fibrin matrices on the exposed wound bed (yellow arrows in Supplemental Figure S2c) and the intradermal location of the injected gels (yellow arrows in Supplemental Figure S2d). Further, injected fibrin gels showed a preferential

localization in the interstitial connective tissue (ICT) below the PC muscle (Supplemental Figure S2d).

Intradermal delivery of TG-VEGF and TG-PDGF-BB-decorated fibrin accelerates wound closure versus layering on the wound bed

Based on our previous results,[12] full-thickness back-skin wounds of db/db mice were treated with fibrin hydrogels decorated with $100\,\mu g/mL$ of murine TG-VEGF$_{164}$ together with $10\,\mu g/mL$ of murine TG-PDGF-BB or fibrin only as control. Fibrin hydrogels were polymerized directly on the wound bed (VP-layer = VEGF and PDGF-BB layering, or F-layer = fibrin only layering) or injected intradermally at the four cardinal points of the wound (VP-4inj = VEGF and PDGF-BB 4 injections, or F-4inj = fibrin only 4 injections). No mice experienced any adverse reaction during the entire experiment duration, including wound inflammation, infection or necrosis, nor significant changes in body weight were observed.

The wound sizes were measured on the day of wounding and after 4 and 8 days to quantify the percentage of wound closure over time. Between 4 and 8 days after wounding, factor-decorated fibrin hydrogels were more effective than control hydrogels, regardless of delivery route (8 days: VP-layer = $54.7 \pm 8.3\%$ vs F-layer = $29.2 \pm 8.9\%$ and VP-4inj = $79.6 \pm 3.1\%$ vs F-4inj = $56.5 \pm 6.4\%$, $p < 0.05$ for both comparisons; Figure 1(a)–(f)). However, treatment by intradermal injection led to significantly faster wound closure at day 8 compared with gel layering (VP-4inj = $79.6 \pm 3.1\%$ vs VP-layer = $54.7 \pm 8.3\%$, $p < 0.05$; Figure 1(e) and (f)). Re-epithelialization, that is the process of covering and repairing denuded epithelial surface by proliferation and differentiation of epithelial stem cells with lateral migration of their progeny, is the defining parameter of successful wound healing.[25] Quantification of tissues harvested 7 days after treatment showed that intradermal injection of VEGF and PDGF-BB-decorated fibrin significantly improved by almost two-fold the extent of re-epithelialization compared with topical treatment (VP-4inj = $81.7 \pm 11.9\%$ vs VP-layer = $44.7 \pm 6.8\%$ $p < 0.01$; Figure 1(g)). Therefore, targeting the undamaged dermis around the wounds with VEGF and PDGF-BB-decorated fibrin hydrogels significantly accelerates the healing process compared to the same treatment applied directly on the wound bed.

Intradermal treatment with TG-VEGF and TG-PDGF-BB-decorated fibrin stimulates microvascular angiogenesis and arteriogenesis around the wound

In order to distinguish the angiogenesis and arteriogenesis induced either in the center or in the periphery of the wound by the two alternative delivery routes, a standardized analysis of the tissue sections was performed

(Supplemental Figure S3). Cryosections were taken from the mid-portion of wound tissues 7 days after treatment, immunostained and images of the whole section were acquired. One fixed area of 800-μm width was chosen to cover the central portion of the wounds, while two other areas were defined, starting at the histologically visible interruption of the PC muscle and extending laterally for 2 mm on each side of the wound, covering the area of injection of fibrin. Localized areas of increased vascular density were visible in all samples, while delivered fibrin was completely degraded by 7 days. In order to evaluate the global effect of treatments, the total surface of these areas was quantified separately from the vascular density within, and quantifications were performed by blinded operators to avoid any bias.

As expected, the total angiogenic area in the peripheral zone around the wounds was markedly increased by the intradermal injection of VEGF + PDGF-decorated fibrin hydrogel compared with its layering on the wound bed (Figure 2(a)–(d) and (i): total angiogenic area-periphery VP-4inj = $454.1 \pm 80.4\,\mu m^2$ vs VP-layer = $94.7 \pm 30.3\,\mu m^2$; $p < 0.05$; $n = 4$). In contrast, in the wound centers layering of VEGF + PDGF-decorated hydrogels did not cause a significant increase in total angiogenic area compared to intradermal injections around the edges (Figure 2(e)–(h) and (j)).

The density of vascular growth within the identified angiogenic areas was quantified by measuring VLD, defined as the total length of vessels in a given area. VLD within the angiogenic areas was similar among all experimental conditions both in the periphery (Figure 3(a)–(e)) and in the center of the wounds (Figure 3(g)–(k)). On the other hand, the total amount of vascular growth is indicated by the total vessel length (TVL), that is the VLD within the areas of effect multiplied by the total angiogenic area of effect in each sample. In the peripheral areas around the wounds, TVL was significantly increased by intradermal injections of VEGF + PDGF-decorated fibrin compared to its layering on the wound beds (Figure 3(f); VP-4inj = 16.2 ± 2.9 mm vs VP-layer = 2.0 ± 0.7 mm, $p < 0.01$), whereas neither treatment significantly increased TVL in the center of the wounds (Figure 3(l)).

Arteriogenesis takes place adjacent to areas of angiogenesis.[12,26] Therefore, the density and the total amount of induced arterioles—defined as vessels larger than capillaries (diameter $\geqslant 15\,\mu$m) associated with α-SMA + smooth muscle coat—were quantified in a fixed radius of 500 μm surrounding all the angiogenic areas (7 days, arteriole diameters: F-layer = $23.5 \pm 1.9\,\mu$m; F-4inj = $26.2 \pm 0.4\,\mu$m; VP-layer = $26.7 \pm 2.7\,\mu$m; VP-4inj = $31.1 \pm 1.4\,\mu$m; p = n.s.).

Interestingly, the arteriolar density was not significantly different among all conditions both in the periphery and the center of the wounds (Figure 3(m) and (n)), consistently with the similar density of micro-vascular networks within the angiogenic areas (Figure 3(e) and (k)). However, the total amount of induced arterioles was markedly increased in the peripheral areas around the wounds by
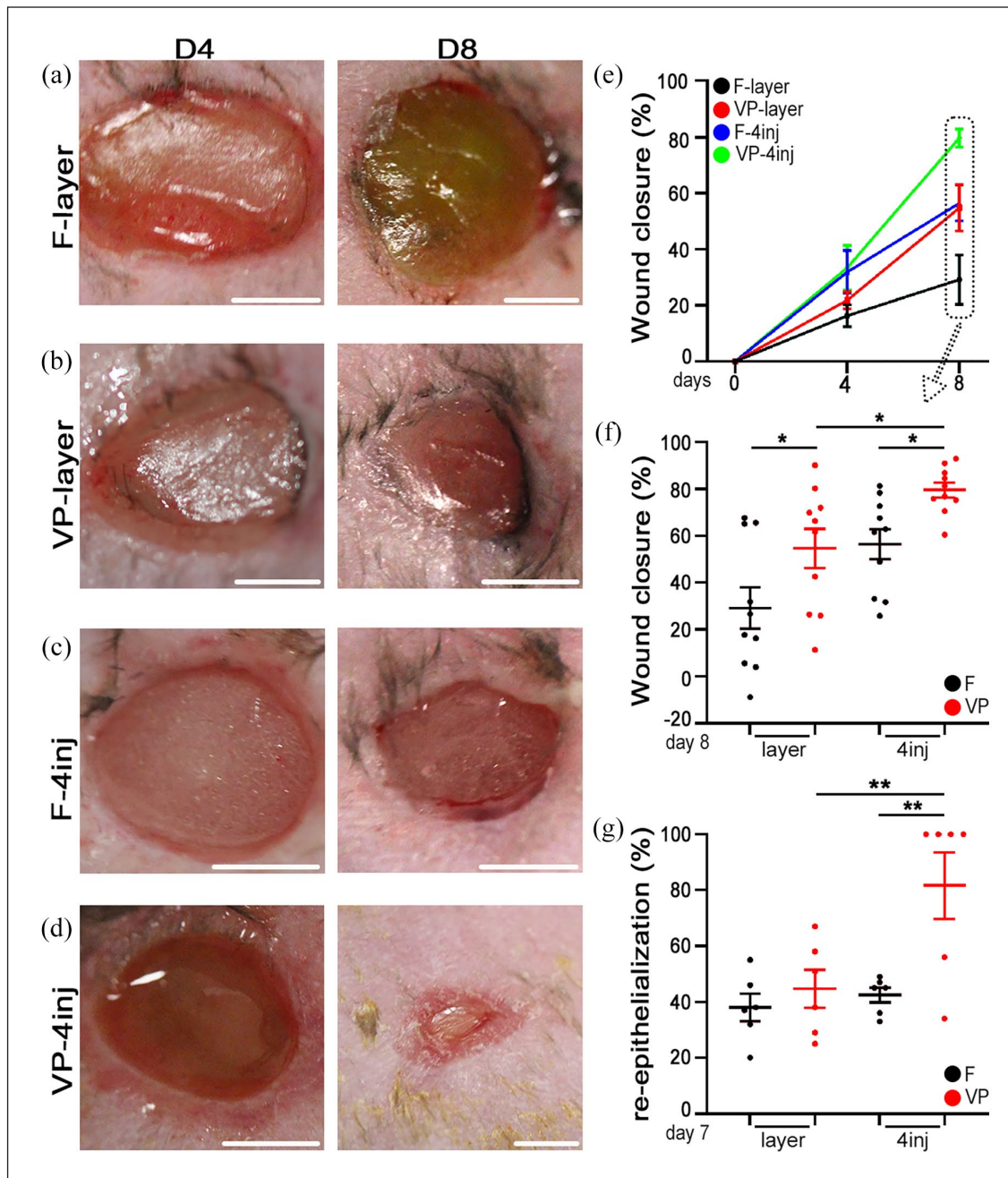
Figure 1. Intradermal treatment with TG-VEGF+TG-PDGF-BB-decorated fibrin accelerates wound healing. (a–d) Full-thickness back-skin wounds of diabetic db/db mice were treated with fibrin gels containing 100 μg/mL TG-VEGF-A + 10 μg/mL of TG-PDGF-BB (VP) or no growth factors (fibrin alone controls, F), which were either layered on the exposed wound bed ((a and b), -layer) or divided in 4 intradermal injections around the wound rim ((c and d), -4inj). Images show the wounds 4 and 8 days after treatment (D4 and D8, respectively). (e and f) Quantification of the percentage of wound closure over time (e), and showing the individual measurements at day 8 as a scatter plot (f), both with mean ± SEM (n = 10 wounds per time-point per group). (g) Quantification of re-epithelialization 7 days after treatment by histomorphometric analysis of H&E-stained cryosections, showing the individual measurements with mean ±SEM (n = 6 wounds per group). *p < 0.05, **p < 0.01 for the indicated pairwise comparisons (one-way ANOVA with Holm-Sidak multiple comparisons test). Scale bars = 2 mm in all panels. F-layer = control fibrin layering; VP-layer = VEGF-A+PDGF-BB fibrin layering; F-4inj = control fibrin 4 injections; VP-4inj = VEGF-A+PDGF-BB fibrin 4 injections.

intradermal injections of TG-VEGF and TG-PDGF-BB-fibrin compared with its layering on the wound beds (Figure 3(o): total arterioles/sample VP-4inj = 12.8 ± 1.6 vs VP-layer = 5.0 ± 1.8, p < 0.05; n = 4–6), whereas neither treatment significantly increased arteriole formation in the center of the wounds (Figure 3(p)).
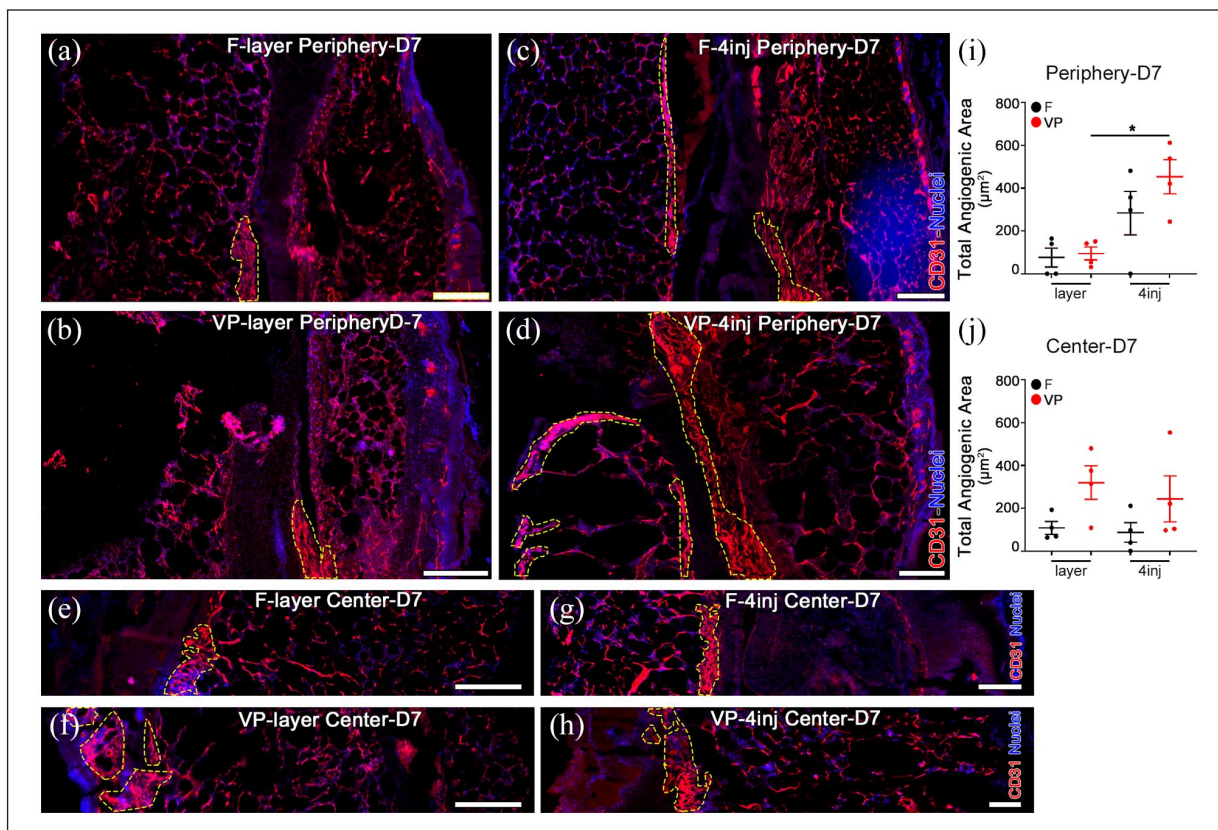
Figure 2. Intradermal treatment with TG-VEGF+TG-PDGF-BB-decorated fibrin stimulates angiogenesis. (a–h) Immunostaining with antibodies against CD31 (endothelial cells, red) and DAPI (nuclei, blue) on cryosections of back skin wounds 7 days after treatment. Images show the angiogenic effects in the peripheral areas ((a–d) Periphery) or in the wound center ((e–h), Center). Angiogenic areas are marked by yellow lines. (i and j) Total angiogenic areas were quantified separately in the periphery (i) or in the center (j) of the wounds. The scatter plots show individual measurements with mean ± SEM (n = 4). *p < 0.05 (one-way ANOVA with Holm-Sidak multiple comparisons test). Scale bars = 500 μm in all panels. F = control fibrin; VP = VEGF-A+PDGF-BB fibrin.

These results show that targeting the normal tissue around the wounds with intradermal delivery of TG-VEGF and TG-PDGF-BB was more effective than layering the growth factors directly on the wound bed in promoting both global vascular growth and arteriogenesis.

Doubling the dose of intradermal injections does not further improve wound healing, angiogenesis and arteriogenesis

As shown in Supplemental Figure S2b, 4 intradermal injections at the cardinal points did not occupy the entire available area around the wound rim. Therefore, a dose escalation experiment was performed to assess if the efficacy of intradermal treatment could be further improved by 8 injections of 21.5 μL each, which was the maximum number compatible with the available space. As shown in Figure 4(a)–(d), 8 injections of factor-decorated fibrin matrices accelerated wound healing by 8 days compared with both 8 injections of control fibrin and gel layering, but to a similar extent as the 4-injection condition (Figure 4(c)

and (d): VP–8inj = 76.0 ± 3.3% vs VP-layer = 54.7 ± 8.3% and vs F–8inj = 53.9 ± 5.0%, p < 0.05 for both comparisons; vs VP-4inj = 79.6 ± 3.1%, p = n.s.; n = 10). Also, after 7 days the VP-8inj treatment did not increase the extent of re-epithelialization more efficiently than the VP-4inj condition (Figure 4(e): VP–8inj = 63.4 ± 12.2% vs VP–4inj = 81.7 ± 11.9% p = n.s.; n = 6).

At day 7 the amount of angiogenesis induced by the different conditions was quantified in the center and periphery of the wounds, as described above. The angiogenic effects of VP-8inj (Figure 5(a)–(d)) were induced over significantly larger areas around the wound rim compared to both its layering on the wound bed and 8 injections of fibrin alone, but similar to the effect of 4 injections of VEGF+PDGF fibrin (Figure 5(e): total angiogenic area VP-8inj = 560.8 ± 99.9 mm² vs F-8inj = 93.3 ± 37.2 mm² and vs VP-layer = 94.7 ± 30.3 mm², p < 0.01 for both comparison; and vs VP-4inj = 454.1 ± 80.4 mm², p = n.s.; n = 4). On the other hand, the total angiogenic area in the center of the wounds was not significantly increased by any treatment (Figure 5(f)). Within the angiogenic areas, VLD was similar among

all conditions in the periphery, while in the center of the wounds it was moderately greater with 4 intradermal injections than with gel layering (Figure 6(a)–(f)). However, due to the significantly more widespread areas of effect induced by intradermal injections, the total amount of vascular growth (TVL) in the peripheral areas was increased by about eightfold by 8 injections of factor-decorated fibrin compared with its layering or 8 injections of control fibrin, but was

similar to the effect of 4 intradermal injections of factor-decorated fibrin (Figure 6(g): VP-8inj = 16.6 ± 2.6 vs F-8inj = 2.4 ± 0.9 mm vs VP-layer = 2.0 ± 0.7, $p < 0.01$ for both comparisons, and vs VP–4inj = 16.2 ± 2.9 mm, p = n.s.; n = 4). Again, the TVL in the center of the wound was not significantly increased by any treatment (Figure 6(h)).

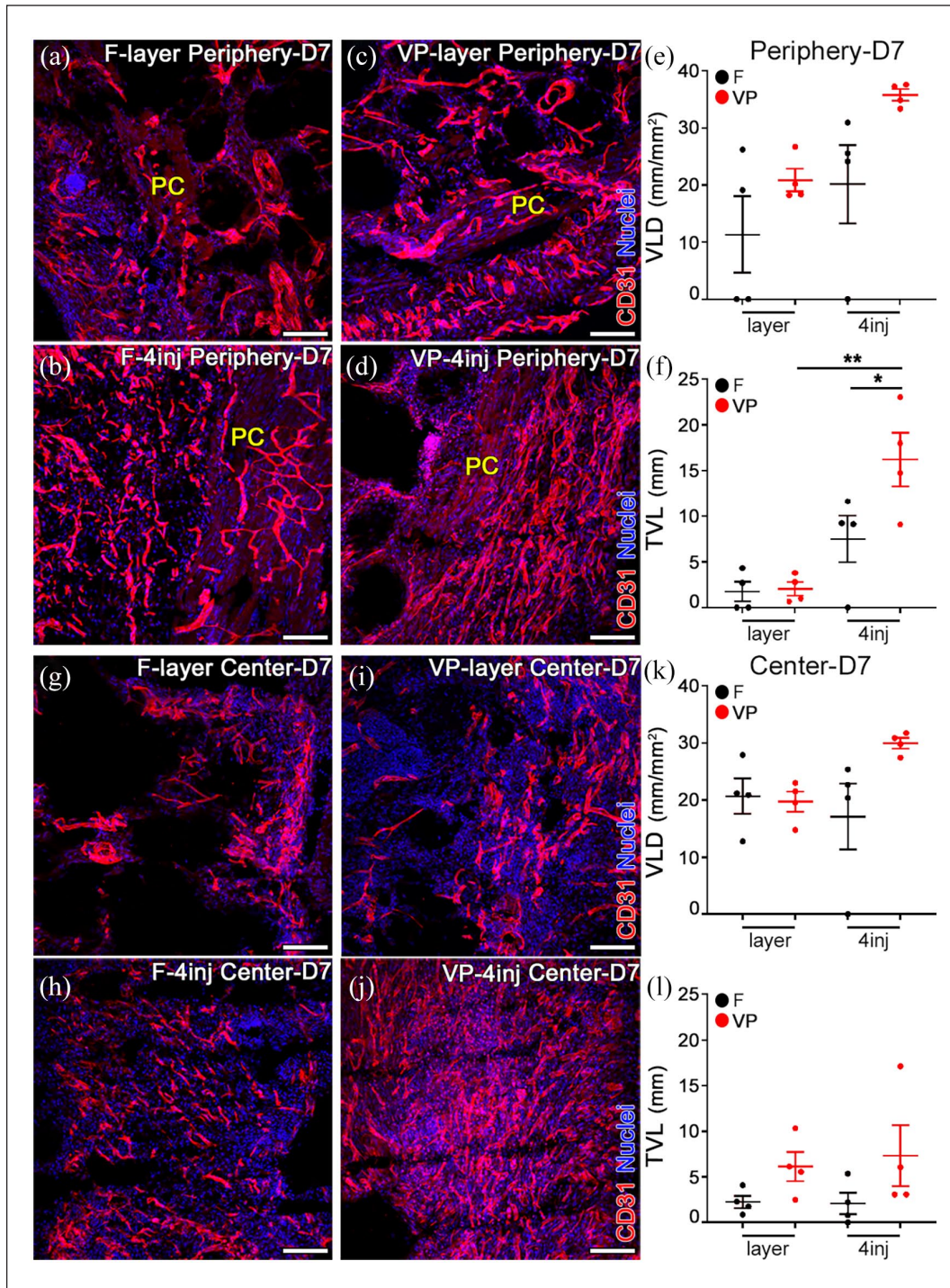Arteriole diameters were quantified in peri-angiogenic areas (7 days, arteriole diameters: F-8inj = 23.7 ± 2.5 µm;

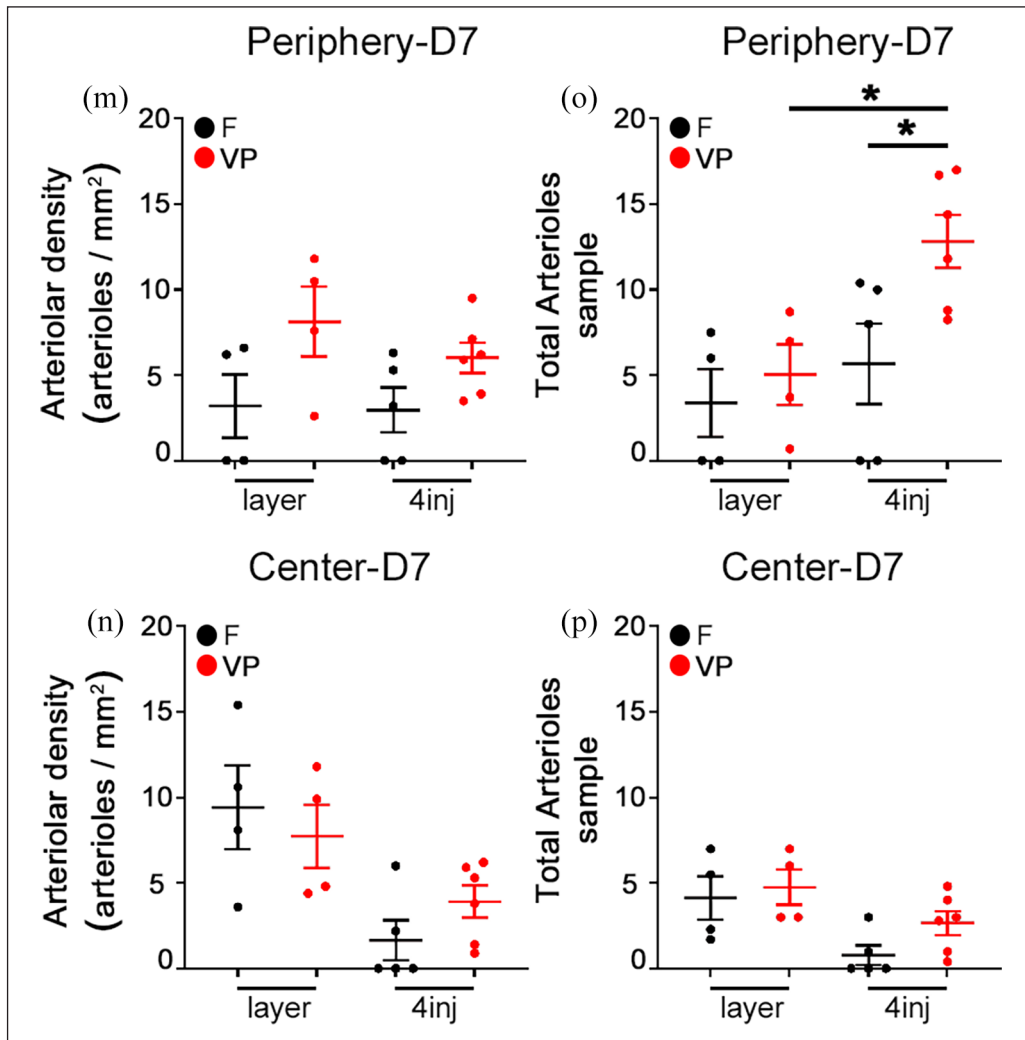

Figure 3. *(Continued)*

Figure 3. Intradermal treatment is more effective to promote total microvascular and arterial growth than topical delivery. Immunostaining for CD31 (endothelial cells, red) and with DAPI (nuclei, blue) on cryosections of back skin wounds 7 days after treatment. Images show the microvascular networks inside angiogenic areas in the periphery ((a–d), Periphery) or in the wound center ((g–j), Center). PC: panniculus carnosus muscle. (e, f, k and l) Microvessels were quantified in the angiogenic areas identified in Figure 2 and expressed as Vessel Length Density (VLD) or Total Vessel Length (TVL) in the peripheral areas (e and f) or in the wound center (k and l). (m–p) Quantification of the arteriolar density adjacent to the angiogenic areas (m and n) and of the total number of arterioles (o and p) in the periphery and center of the wounds. The scatter plots show individual measurements with mean $\pm$ SEM ($n = 4$–6). *$p < 0.05$, **$p < 0.01$ (one-way ANOVA with Holm-Sidak multiple comparisons test). Scale bars = 500 μm in all panels. F = control fibrin; VP = VEGF-A + PDGF-BB fibrin.

VP-8inj = 30.4 $\pm$ 3.6 μm; p = n.s.). Similarly to the results shown in Figure 3, the density of arterioles around the angiogenic areas was similar in all treatments (Figure 6(i) and (j)), but the total amount of induced arterioles was markedly increased in the peripheral areas around the wounds by both 8 and 4 intradermal injections of VEGF + PDGF-decorated fibrin compared with its layering on the wound beds or 8 injections of control fibrin (Figure 6(k): total arterioles/sample VP-8inj = 15.2 $\pm$ 1.8 vs F-8inj = 4.2 $\pm$ 2.3, $p < 0.01$, and vs VP-layer = 5.0 $\pm$ 1.8, $p < 0.05$, and vs VP-4inj = 12.8 $\pm$ 1.6, p = n.s.; $n = 4$). No mode of delivery of factor-decorated fibrin significantly

increased arteriole formation in the center of the wounds compared to the others (Figure 6(l)). Therefore, these data indicate that the maximal efficacy was reached already with 4 intradermal injections of TG-VEGF + TG-PDGF-decorated fibrin around the wound.

Discussion

Here we found that a specific pro-arteriogenic treatment, based on fibrin matrices decorated with high doses of engineered recombinant VEGF and PDGF-BB, efficiently accelerates wound closure in diabetic and obese db/db
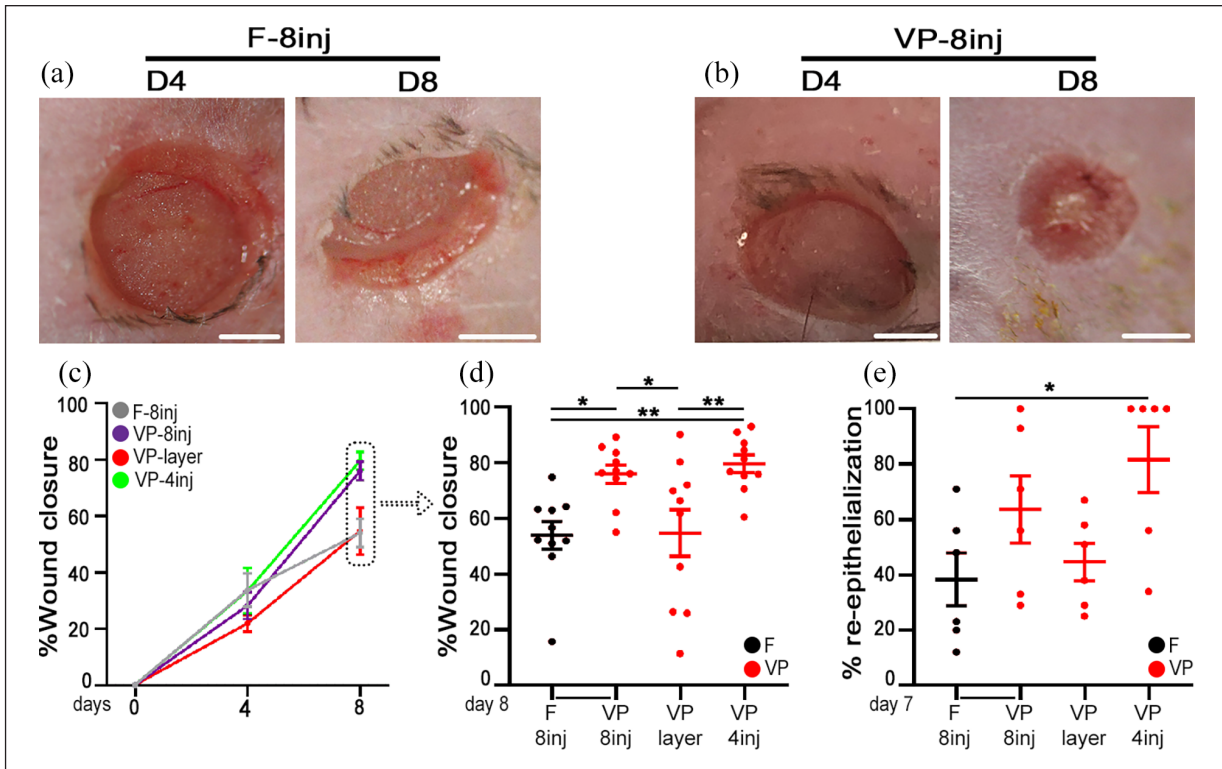
Figure 4. Efficacy of intradermal treatment with TG-VEGF+TG-PDGF-BB-decorated fibrin is not further improved by a double dose. (a and b) Full-thickness back-skin wounds treated with 8 intradermal injections of either control fibrin (F-8inj) or TG-VEGF+TG-PDGF-BB-decorated fibrin (VP-8inj), 4 and 8 days after treatment (D4 and D8, respectively). (c and d) Quantification of the percentage of wound closure over time (c), and showing the individual measurements of each wounded area at Day 8 as a scatter plot (d), both with mean ± SEM. (e) Quantification of the extent of re-epithelialization 7 days after treatment by histomorphometric analysis of H&E-stained cryosections. $*p < 0.05$, $**p < 0.01$ for the indicated pairwise comparisons (one-way ANOVA with Holm-Sidak multiple comparisons test; $n = 10$ wounds/time-point/group in (c and d) and $n = 6$ wounds/group in (e). Scale bars = 2 mm in all panels. F-8inj = control fibrin 8 injections; VP-8inj = VEGF+PDGFBB fibrin 8 injections; VP-layer = VEGF-A+PDGF-BB fibrin layering; VP-4inj = VEGF+PDGFBB fibrin 4 injections.

mice, with robust microvascular growth accompanied by a marked increase in feeding arterioles. In particular, targeting the undamaged tissue around the wound by intradermal injections is significantly more effective than delivering the same treatment directly onto the damaged wound bed.

Even though animals do not develop chronic wounds that fully resemble those arising in human patients, animal models are crucial to provide critical insights into the mechanistic and therapeutic aspects of wound healing. Biological variables such as age, sex and wound location contribute to the variability in the outcomes of preclinical studies using animal models for wound healing.[27] The monogenic diabetic db/db mouse is a well-established and widely used experimental model of Type 2 diabetes,[13] contrary to other drug-induced models, for example, by Streptozotocin treatment, that cause an acute destruction of insulin-producing cells in the pancreatic islets and are more similar to the pathogenesis of Type 1 diabetes.[27] Although the specific autosomal recessive mutation in the leptin receptor is not usually present in human Type 2

diabetes, this model reproduces many features of the human disease through the obesity-induced peripheral insulin resistance, which is an important pathogenic mechanism of human Type 2 diabetes.[28] Further, wound contraction, the physiological mechanism of wound healing in rodents, is different from the human healing pathway of epithelialization and granulation. However, this strain heals wounds mainly by the formation of granulation tissue rather than by contraction.[29]

Recombinant VEGF and PDGF-BB proteins have been previously employed clinically to accelerate the healing of chronic wounds, as single drugs and applied as topical gels, but have shown limited efficacy.[30] In particular, a topical gel formulation of recombinant human (rh) PDGF-BB (Becaplermin, Regranex) has been approved by the FDA for the treatment of DFUs,[31–34] but subsequently failed to yield evidence-based efficacy in clinical practice[35,36] and its use remains restricted because of uncertainties regarding its time of application as well as its safety profile.[37] Additionally, the efficacy of topical gel formulations has been found to become limited with increasing
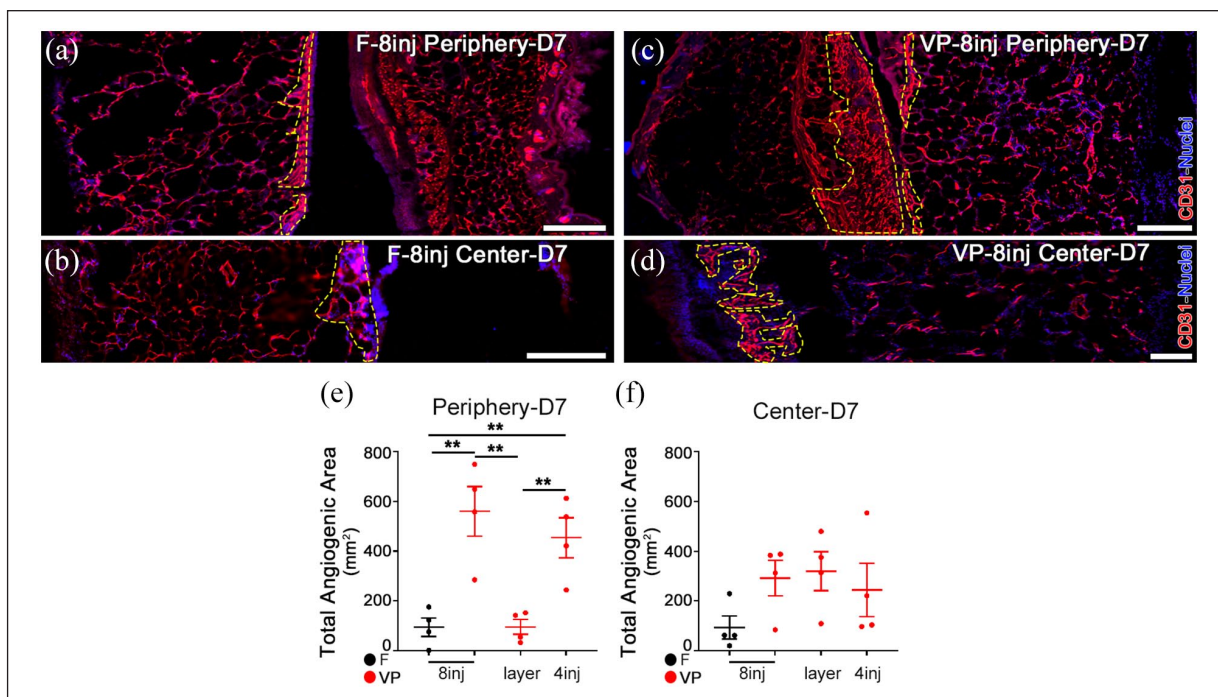
Figure 5. Total angiogenesis is maximal with 4 intradermal injections of TG-VEGF+TG-PDGF-BB-decorated fibrin. (a–d) Immunostaining with antibodies against CD31 (endothelial cells, red) and with DAPI (nuclei, blue) on cryosections of back skin wounds 7 days after treatment with 8 intradermal injections of control fibrin (F-8inj) or TG-VEGF+TG-PDGF-BB-decorated fibrin (VP-8inj). Angiogenic areas are marked by yellow lines. (e and f) Quantification of the total angiogenic area in the peripheral areas ((e), Periphery) or in the wound center ((f), Center). Scatter plots show individual values with mean $\pm$ SEM ($n = 4$). **$p < 0.01$ (one-way ANOVA with Holm-Sidak multiple comparisons test). Scale bars = 500 μm in all panels. F = control fibrin; VP = VEGF-A+PDGF-BB fibrin.

severity of ulcers, as the growth factors undergo proteolytic breakdown with consequent inadequate reach to the deeper wound layers.[35,36] Topical therapy of DFUs with recombinant human VEGF (rh-VEGF, Telbermin) has also been met with limited clinical success. In fact, although phase-1 trials showed positive trends suggestive of potential biological activity in terms of incidence of complete ulcer healing and time to complete ulcer healing,[38] the drug was abandoned after Phase-2 clinical trials and clinical benefit has yet to be established.[39] A combination of the two factors has not been tested clinically and the healing of chronic wounds in diabetic patients remains a significant unmet clinical need.

Stimulation of the growth of new blood vessels supplying the wound is essential to provide for the metabolic needs of the healing response.[6] While the growth of microvascular networks can facilitate metabolic exchanges, efficient improvement of blood perfusion in the wound tissue requires the induction of new bridging arteries recruiting flow from the deeper circulation. This process is named arteriogenesis and is distinct from angiogenesis, as it takes place through enlargement and remodeling of small pre-existing vessels.[8] From a molecular standpoint, the two processes are also regulated differently. In fact, while moderate doses of VEGF alone direct efficient angiogenic

microvascular growth that is also accompanied by the formation of smooth muscle-coated larger arterioles adjacent to it,[26] the process of arteriogenesis actually benefits from the delivery of higher doses of VEGF in combination with PDGF-BB.[11] These high doses of VEGF would lead to aberrant angiogenesis when delivered alone, but the co-delivery of PDGF-BB prevents this outcome and ensures instead the growth of dense networks of only normal capillaries accompanied by abundant feeding arteries.[10,11] Therefore, the dose and combination of factors used here were chosen based on these previous findings showing optimal arteriogenic effect in skeletal muscle, and their confirmation in the specific target tissue of skin in diabetic and obese db/db mice.[12]

The data presented here show that intradermal delivery of TG-VEGF and TG-PDGF-BB to the undamaged tissue around the wounds was significantly more effective than the same treatment applied topically on the wound bed to (1) accelerate the closure of the wounds and (2) robustly increase both micro-vascular angiogenesis and feeding arteriogenesis. The clear difference in efficacy of the same treatment at the same dose simply delivered by two distinct routes may be explained by two orders of considerations: (1) the inflammatory environment of the wound bed, and (2) the vascular anatomy of skin. In fact, physiological
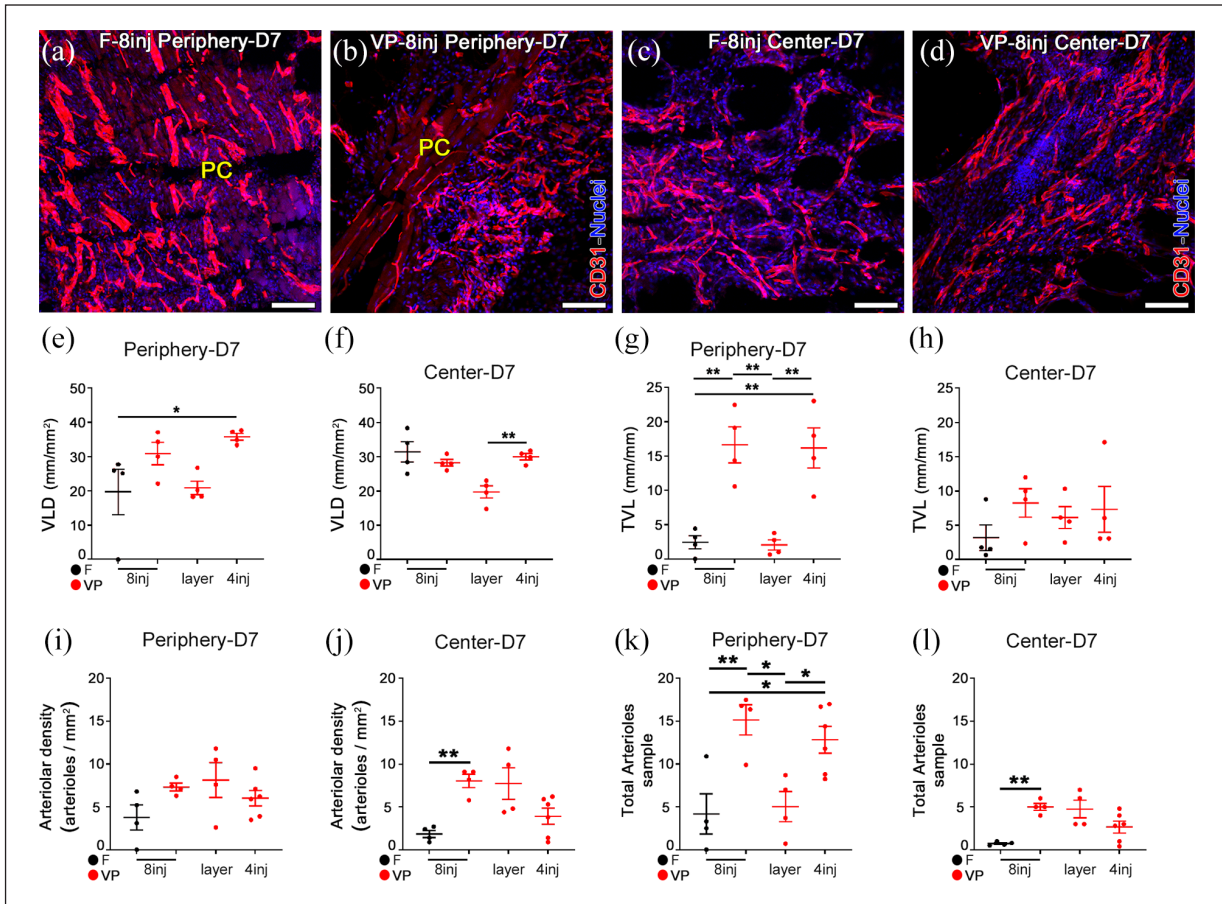
Figure 6. Total microvascular and arterial growth are maximal with 4 intradermal injections of TG-VEGF+TG-PDGF-BB-decorated fibrin. (a–d) Immunostaining with antibodies against CD31 (endothelial cells, red) and with DAPI (nuclei, blue) on cryosections of back skin wounds 7 days after treatment with 8 intradermal injections of control fibrin (F-8inj) or TG-VEGF+TG-PDGF-BB-decorated fibrin (VP-8inj). PC = Panniculus Carnosus muscle. (e–h) Quantification of Vessel Length Density (VLD, (e and f)) and Total Vessel Length (TVL, (g and h)) in the peripheral areas (Periphery) or in the wound center (Center). (i–l) Quantification of the arteriolar density adjacent to the angiogenic areas (i and j) and of the total number of arterioles (k and l) in the periphery and center of the wounds. Scatter plots show individual values with mean ± SEM (n = 4–6/group). $*p < 0.05$, $**p < 0.01$ (one-way ANOVA with Holm-Sidak multiple comparisons test). Scale bars = 100 μm in all panels. F = control fibrin; VP = VEGF-A+PDGF-BB fibrin.

wound healing proceeds normally through four phases, that is coagulation, inflammation, migration/proliferation of regenerating cells and remodeling/resolution,[40] whereas chronic wounds remain stalled in a state of persistent inflammation. This is characterized by abundant levels of proteases, which can cause the rapid degradation of the delivered growth factors and reduce their biological activity. For example, neutrophil elastase, which is produced at high levels in chronic wounds, is capable of cleaving PDGF-BB and inhibiting its biological activity.[41] Additionally, plasmin-mediated VEGF degradation has been found to be significantly increased at the wound site in db/db mice and in wound fluid collected from non-healing human chronic wounds.[42,43] On the other hand, a proteolysis-resistant form of VEGF was shown to display increased stability[44] and to accelerate wound closure in db/db mice.[43]

Considering vascular anatomy, the skin is supplied by two arterio-venous plexuses that run horizontally along the surface: the superficial plexus in the papillary dermis just below the epidermal layer, and the deep plexus at the dermal-subcutaneous interface. The deep plexus consists of larger arterioles that receive flow directly from the main arteries running in the underlying muscle or fat, and supply the superficial plexus and the microvascular networks emanating from it.[45] Both these plexuses are destroyed in the bed of a chronic diabetic ulcer, as well as in the murine full-thickness wound model used experimentally, but they are preserved in the undamaged dermal-subcutaneous layers around the wound. Therefore, intradermal injections of TG-VEGF+TG-PDGF-BB-decorated hydrogel place the arteriogenic factors in direct anatomical proximity to their biological target, that is the arteriole plexus connecting to the deep blood supply. The improved vascularization

around the wound is in turn ideally positioned to supply the epidermal progenitors and other regenerative cells that proceed centripetally from the wound rim toward the center.

In order to overcome the limitations of recombinant growth factors delivery to treat DFUs, specific areas for improvement have been identified, including the following: (1) protecting the growth factors from degradation, (2) allowing controllable release, and (3) reducing the frequency of administration.[30] The fibrin hydrogel-based platform that was employed here provides several desirable features for clinical translation addressing these issues. In fact, covalent cross-linking of the recombinant factors to the fibrin matrix completely shields them from degradation until release by enzymatic cleavage of the matrix itself.[46] Further, the dose and duration of release are highly tunable by controlling the degradation rate of the matrix by incorporating a TG-version of the fibrinolysis inhibitor aprotinin, different concentrations of which can match the needs of different tissue inflammation levels.[14] As shown here, repeated application was not necessary to achieve the pro-angiogenic and pro-arteriogenic effects and accelerate wound healing, even without aprotinin addition. However, in case clinical conditions demanded a longer duration of release, aprotinin incorporation has been shown to prolong fibrin matrix persistence up to 4 weeks.[14] Lastly, fibrinogen is routinely used as biological glue in surgical procedures (e.g. TISSEEL®), thereby facilitating a regulatory approval for clinical use.

On the other hand, a growing body of evidence suggests that cell therapy, mainly based on mesenchymal progenitors from a variety of tissue sources and circulating endothelial progenitor cells, can also be effective in accelerating diabetic wound healing.[47] The principal mechanism of action is believed to rely on their rich production of paracrine factors, which both stimulate angiogenesis and modulate the local inflammatory response, thereby restarting the healing process that is stalled in a chronic inflammatory state.[7] Further, endothelial progenitor cells may directly contribute to new blood vessel formation. Whether the combination of cell-based and factor-based therapeutic strategies may be synergistic remains to be investigated and is an interesting line of future research.

In conclusion, this work shows that a specific pro-arteriogenic treatment, comprised of the co-delivery of high doses of TG-VEGF and TG-PDGF-BB within fibrin by intradermal injection in the undamaged tissue around the wound, is superior to application of the factors onto the wound bed to accelerate wound healing in diabetic mice and holds promise for clinical translation.

Acknowledgements

Author contributions

Conception and design: A.B., R.G.-B., E.M., L.G., T.W., J.A.H., P.S.B.; Acquisition, analysis and interpretation of data: R.D'A., C.M., A.U., A.G., N.D.M., P.S.B., R.G.B., A.B.; Manuscript draft preparation: R.D'A., C.M.; Editing and revision: A.B., R.G.-B., E.M., L.G., T.W., J.A.H., P.S.B., N.D.M., A.G., A.U. All Authors have approved the submitted manuscript version.

Declaration of conflicting interests

The author(s) declared the following potential conflicts of interest with respect to the research, authorship, and/or publication of this article: The fibrin gel immobilization scheme is the subject of patents upon which J.A.H. is named as inventor and has been licensed by a company in which J.A.H. is a shareholder.

Funding

Ethical approval

Animals were treated in accordance with Swiss Federal guidelines for animal welfare and the study protocol was approved by the Veterinary Office of the Canton of Basel-Stadt (Basel, Switzerland, Permit 2952).

ORCID iDs

Andrea Banfi https://orcid.org/0000-0001-5737-8811
Roberto Gianni-Barrera https://orcid.org/0000-0001-6303-4513

Supplemental material

Supplemental material for this article is available online.

References

1. Saeedi P, Petersohn I, Salpea P, et al. Global and regional diabetes prevalence estimates for 2019 and projections for 2030 and 2045: Results from the International Diabetes Federation Diabetes Atlas, 9(th) edition. *Diabetes Res Clin Pract* 2019; 157: 107843.

2. Zhang P, Lu J, Jing Y, et al. Global epidemiology of diabetic foot ulceration: a systematic review and meta-analysis. *Ann Med* 2017; 49: 106–116.

3. Armstrong DG, Boulton AJM and Bus SA. Diabetic foot ulcers and their recurrence. *N Engl J Med* 2017; 376: 2367–2375.

4. Saluja S, Anderson SG, Hambleton I, et al. Foot ulceration and its association with mortality in diabetes mellitus: a meta-analysis. *Diabet Med* 2020; 37: 211–218.

5. Altabas V. Diabetes, endothelial dysfunction, and vascular repair: what should a diabetologist keep his eye on? *Int J Endocrinol* 2015; 2015: 848272.

6. Okonkwo UA and DiPietro LA. Diabetes and wound angiogenesis. *Int J Mol Sci* 2017; 18: 1419.

7. Otero-Viñas M and Falanga V. Mesenchymal stem cells in chronic wounds: the spectrum from basic to advanced therapy. *Adv Wound Care* 2016; 5: 149–163.

8. Annex BH. Therapeutic angiogenesis for critical limb ischaemia. *Nat Rev Cardiol* 2013; 10: 387–396.

9. Uccelli A, Wolff T, Valente P, et al. Vascular endothelial growth factor biology for regenerative angiogenesis. *Swiss Med Wkly* 2019; 149: w20011.

10. Banfi A, von Degenfeld G, Gianni-Barrera R, et al. Therapeutic angiogenesis due to balanced single-vector delivery of VEGF and PDGF-BB. *FASEB J* 2012; 26: 2486–2497.

11. Gianni-Barrera R, Burger M, Wolff T, et al. Long-term safety and stability of angiogenesis induced by balanced single-vector co-expression of PDGF-BB and VEGF164 in skeletal muscle. *Sci Rep* 2016; 6: 21546.

12. Certelli A, Valente P, Uccelli A, et al. Robust angiogenesis and arteriogenesis in the skin of diabetic mice by transient delivery of engineered VEGF and PDGF-BB proteins in fibrin hydrogels. *Front Bioeng Biotechnol* 2021; 9: 688467.

13. Sullivan SR, Underwood RA, Gibran NS, et al. Validation of a model for the study of multiple wounds in the diabetic mouse (db/db). *Plast Reconstr Surg* 2004; 113: 953–960.

14. Sacchi V, Mittermayr R, Hartinger J, et al. Long-lasting fibrin matrices ensure stable and functional angiogenesis by highly tunable, sustained delivery of recombinant VEGF164. *Proc Natl Acad Sci U S A* 2014; 111: 6952–6957.

15. Everett E and Mathioudakis N. Update on management of diabetic foot ulcers. *Ann N Y Acad Sci* 2018; 1411: 153–165.

16. Gainza G, Villullas S, Pedraz JL, et al. Advances in drug delivery systems (DDSs) to release growth factors for wound healing and skin regeneration. *Nanomed* 2015; 11: 1551–1573.

17. Zhao R, Liang H, Clarke E, et al. Inflammation in chronic wounds. *Int J Mol Sci* 2016; 17(12): 16.

18. Zisch AH, Schenk U, Schense JC, et al. Covalently conjugated VEGF–fibrin matrices for endothelialization. *J Control Release* 2001; 72: 101–113.

19. von Degenfeld G, Banfi A, Springer ML, et al. Microenvironmental VEGF distribution is critical for stable and functional vessel growth in ischemia. *FASEB J* 2006; 20: 2657–2659.

20. Ozawa CR, Banfi A, Glazer NL, et al. Microenvironmental VEGF concentration, not total dose, determines a threshold between normal and aberrant angiogenesis. *J Clin Invest* 2004; 113: 516–527.

21. Martino MM, Tortelli F, Mochizuki M, et al. Engineering the growth factor microenvironment with fibronectin domains to promote wound and bone tissue healing. *Sci Transl Med* 2011; 3: 100ra89.

22. Greer JJ, Ware DP and Lefer DJ. Myocardial infarction and heart failure in the db/db diabetic mouse. *Am J Physiol Heart Circ Physiol* 2006; 290: H146–H153.

23. Hummel KP, Dickie MM and Coleman DL. Diabetes, a new mutation in the mouse. *Science* 1966; 153: 1127–1128.

24. FDA Wound Healing Clinical Focus Group. Guidance for industry: chronic cutaneous ulcer and burn wounds-developing products for treatment. *Wound Repair Regen* 2001; 9: 258–268.

25. Pastar I, Stojadinovic O, Yin NC, et al. Epithelialization in Wound Healing: A Comprehensive Review. *Adv Wound Care* 2014; 3: 445–464.

26. Springer ML, Ozawa CR, Banfi A, et al. Localized arteriole formation directly adjacent to the site of VEGF-induced angiogenesis in muscle. *Mol Ther* 2003; 7: 441–449.

27. Elliot S, Wikramanayake TC, Jozic I, et al. A modeling conundrum: murine models for cutaneous wound healing. *J Investig Dermatol* 2018; 138: 736–740.

28. Grada A, Mervis J and Falanga V. Research techniques made simple: animal models of wound healing. *J Investig Dermatol* 2018; 138: 2095–2105.e2091.

29. Davidson JM. Animal models for wound repair. *Arch Dermatol Res* 1998; 290(Suppl l): S1–11.

30. Veith AP, Henderson K, Spencer A, et al. Therapeutic strategies for enhancing angiogenesis in wound healing. *Adv Drug Deliv Rev* 2019; 146: 97–125.

31. Embil JM, Papp K, Sibbald G, et al. Recombinant human platelet-derived growth factor-BB (becaplermin) for healing chronic lower extremity diabetic ulcers: an open-label clinical evaluation of efficacy. *Wound Repair Regen* 2000; 8: 162–168.

32. Margolis DJ, Bartus C, Hoffstad O, et al. Effectiveness of recombinant human platelet-derived growth factor for the treatment of diabetic neuropathic foot ulcers. *Wound Repair Regen* 2005; 13: 531–536.

33. Steed DL. Clinical evaluation of recombinant human platelet – derived growth factor for the treatment of lower extremity diabetic ulcers. *J Vasc Surg* 1995; 21: 71–81; discussion 79-81.

34. Wieman TJ, Smiell JM and Su Y. Efficacy and safety of a topical gel formulation of recombinant human platelet-derived growth factor-BB (becaplermin) in patients with chronic neuropathic diabetic ulcers. A phase III randomized placebo-controlled double-blind study. *Diabetes Care* 1998; 21: 822–827.

35. Eleftheriadou I, Tentolouris A, Tentolouris N, et al. Advancing pharmacotherapy for diabetic foot ulcers. *Expert Opin Pharmacother* 2019; 20: 1153–1160.

36. Papanas N and Maltezos E. Becaplermin gel in the treatment of diabetic neuropathic foot ulcers. *Clin Interv Aging* 2008; 3: 233–240.

37. Papanas N and Maltezos E. Benefit-risk assessment of becaplermin in the treatment of diabetic foot ulcers. *Drug Saf* 2010; 33: 455–461.

38. Hanft JR, Pollak RA, Barbul A, et al. Phase I trial on the safety of topical rhVEGF on chronic neuropathic diabetic foot ulcers. *J Wound Care* 2008; 17: 30–32. 34-37.

39. Whittam AJ, Maan ZN, Duscher D, et al. Challenges and opportunities in drug delivery for Wound Healing. *Adv Wound Care* 2016; 5: 79–88.

40. Falanga V. Wound healing and its impairment in the diabetic foot. *Lancet* 2005; 366: 1736–1743.

41. Yager DR, Chen SM, Ward SI, et al. Ability of chronic wound fluids to degrade peptide growth factors is associated with increased levels of elastase activity and diminished levels of proteinase inhibitors. *Wound Repair Regen* 1997; 5: 23–32.

42. Lauer G, Sollberg S, Cole M, et al. Expression and proteolysis of vascular endothelial growth factor is increased in chronic wounds. *J Investig Dermatol* 2000; 115: 12–18.

43. Roth D, Piekarek M, Paulsson M, et al. Plasmin modulates vascular endothelial growth factor-A-mediated angiogenesis during wound repair. *Am J Pathol* 2006; 168: 670–684.

44. Lauer G, Sollberg S, Cole M, et al. Generation of a novel proteolysis resistant vascular endothelial growth factor165 variant by a site-directed mutation at the plasmin sensitive cleavage site. *FEBS Lett* 2002; 531: 309–313.

45. Liao F, Burns S and Jan YK. Skin blood flow dynamics and its role in pressure ulcers. *J Tissue Viability* 2013; 22: 25–36.

46. Largo RA, Ramakrishnan VM, Marschall JS, et al. Long-term biostability and bioactivity of "fibrin linked" VEGF121in vitro and in vivo. *Biomater Sci* 2014; 2: 581–590.

47. Yu Q, Qiao GH, Wang M, et al. Stem cell-based therapy for diabetic foot ulcers. *Front Cell Dev Biol* 2022; 10: 812262.